CIT-1: A New Molecular Sieve with Intersecting Pores Bounded by 10- and 12-Rings

Raul F. Lobo and Mark E. Davis*,†

Contribution from the Department of Chemical Engineering, California Institute of Technology, Pasadena, California 91125

Received November 28, 1994[⊗]

Abstract: A new borosilicate molecular sieve, CIT-1, is synthesized using *N,N,N*-trimethyl-(−)-*cis*-myrtanylammonium (**I**) hydroxide as the organic structure-directing agent. The material is characterized by synchrotron X-ray powder diffraction (XRD), electron diffraction, solid-state NMR and IR spectroscopies, scanning electron microscopy, and physical adsorption experiments. Rietveld refinement of the synchrotron XRD data (Rp = 9.9%, Rwp = 11.9%) shows that CIT-1 is essentially the pure polymorph B of the molecular sieve SSZ-33 (space group *C2/m*, no. 12, a = 22.6242(10) Å, b = 13.3503 (4) Å, c = 12.3642 (6) Å, and β = 68.913(4)°). CIT-1 is the first synthetic molecular sieve to contain intersecting 10- and 12-ring pores that is not an intergrowth of two different polymorphs. The long-range ordering of CIT-1 is shown to be a direct consequence of the organic structure-directing agent. CIT-1 can be easily prepared and sequential treatments of the calcined form of CIT-1 with aqueous HCl, and aqueous aluminum nitrate remove framework boron and insert aluminum into the structure, respectively. Aluminum-containing CIT-1 is a very active catalyst for the cracking of *n*-butane at 783 K.

Introduction

Zeolites are technologically important materials that have found applications in a wide variety of chemical processes.[1−3] One of the appealing features of these materials is the existence of a direct relationship between the microscopic structure of the crystalline solids and their macroscopic properties.[4] The rationalization of sorptive, catalytic, and ion exchange properties in terms of molecular structure allows for the suggestion of new applications for these materials and drives the search for zeolites with novel structures. The synthesis of SSZ-33,[5] NU-87[6] (or SSZ-37),[7,8] and MCM-22[9] (or SSZ-25)[10] are recent successful examples of the synthesis of new zeolite structures.

New large pore zeolites, those with pores bounded by rings of 12 tetrahedral atoms (T-atoms, e.g., Si, Al, B), from now on denoted 12MR, are of current interest due to their pore size; ~7 Å. Zeolites Y and beta have intersecting 12MR pores and have found application in petrochemical processing as catalysts. Likewise, ZSM-5, an intersecting 10MR zeolite is used quite extensively in shape-selective catalysis, e.g., production of *p*-xylene. It is likely that zeolites with intersecting 10MR and 12MR pores will offer a unique combination of reaction activity, selectivity, and stability not found in other zeolites.[11]

Recently, we reported the structures of SSZ-33 and SSZ-26,[12] the first materials to contain a multidimensional pore system formed by intersecting 10MR and 12MR pores that provide access to the crystal interior through both pore sizes. The structures of SSZ-33 and SSZ-26 can be thought of as members of a family of materials in which the two end members (denoted polymorphs A and B) are formed by the stacking of layers in an ABAB... sequence or an ABCABC... sequence. The framework formed by the ABAB... stacking sequence (polymorph A) is of orthorhombic symmetry, while the framework formed by the ABCABC... stacking sequence (polymorph B) is of monoclinic symmetry. In between these two end member polymorphs, there is a whole family of materials that can be characterized by a fault probability p. The fault probabilities of p = 0% and p = 100% represent the end members polymorph B and polymorph A, respectively. The aluminosilicate SSZ-26 and the borosilicate SSZ-33 are members of this family of materials with fault probabilities of approximately 15% and 30%, respectively.[13]

Like zeolite beta, SSZ-26 and SSZ-33 are likely to show interesting catalytic properties that will not be easily correlated to structural parameters since all three materials are intergrowth structures. A pure phase would greatly assist the determination of structure−catalytic property relationships for this new class of zeolites (with intersecting 10MR and 12MR pores). Here we report on the first pure phase zeolite with intersecting 10MR and 12MR pores that provides molecular access to the crystal interior through the 12MR and 10MR pores. We denote this material as CIT−1 for California Institute of Technology−1.[14]

The synthesis and initial characterization of CIT-1, a novel molecular sieve that has been identified as the ordered polymorph B of the SSZ-33 and SSZ-26 molecular sieves is presented here. Unlike the structure-directing agents used to prepare SSZ-33 and SSZ-26 that require significant preparative steps in their synthesis, the structure-directing agent of CIT-1 can be obtained from suppliers of organic compounds or can be easily prepared from β-pinene. CIT-1 is characterized using synchrotron X-ray powder diffraction (XRD), scanning electron

† Phone: (818) 395-4674. Fax: (818) 568-8743.
* Corresponding author mdavis@macpost.caltech.edu.
⊗ Abstract published in *Advance ACS Abstracts*, March 15, 1995.
(1) Maxwell, I. E.; Stork, W. H. J. *Stud. Surf. Sci. Catal.* **1991**, *58*, 571−630.
(2) Moscou, L. *Stud. Surf. Sci. Catal.* **1991**, *58*, 1−12.
(3) Davis, M. E. *Ind. Eng. Chem. Res.* **1991**, *30*, 1675−1683.
(4) Newsam, J. M. In *Solid State Chemistry: Compounds*; Cheetham, A. K., Day, P., Eds.; Oxford University Press: New York, 1992; Vol. 2.
(5) Zones, S. I. U.S. Patent 4963337, 1990.
(6) Shannon, M. D.; Casci, J. L.; Cox, P. A.; Andrews, S. J. *Nature* **1991**, *353*, 417−420.
(7) Nakagawa, Y. U.S. Patent 5,254,514, 1993.
(8) Nakagawa, Y. *Stud. Surf. Sci. Catal.* **1994**, *84*, 323−330.
(9) Leonowicz, M. E.; Lawton, J. A.; Lawton, S. L.; Rubin, M. K. *Science* **1994**, *264*, 1910−1913.
(10) Zones, S. I., European Pat. Appl. EP 231,019, 1987.
(11) Davis, M. E.; Lobo, R. F. *Chem. Mater.* **1992**, *4*, 756.
(12) Lobo, R. F.; Pan, M.; Chan, I.; Li, H. X.; Medrud, R. C.; Zones, S. I.; Crozier, P. A.; Davis, M. E. *Science* **1993**, *262*, 1543−1546.
(13) Lobo, R. F.; Pan, M.; Chan, I.; Medrud, R. C.; Zones, S. I.; Crozier, P. A.; Davis, M. E. *J. Phys. Chem.* **1994**, *98*, 12040−12052.
(14) Lobo, R. F.; Zones, S. I.; Davis, M. E. *Stud. Sur. Sci. Catal.* **1994**, *84*, 461−468.

0002-7863/95/1517-3766$09.00/0

microscopy (SEM), physical adsorption experiments, solid-state NMR spectroscopy, IR spectroscopy, and electron diffraction (ED). The ED data and a Rietveld refinement of the XRD data from a calcined sample are used to confirm the proposed structure of CIT-1. Also, the catalytic properties of CIT-1 for the cracking of *n*-butane are compared to those of the high-silica zeolites ZSM-5 and beta.

Experimental Section

Synthesis of the Organic Structure-Directing Agents. Synthesis of *N,N,N*-Trimethyl-(−)-cis-myrtanylammonium (I) Hydroxide. A typical synthesis of *N,N,N*-trimethyl-(−)-*cis*-myrtanylammonium is carried out as follows: 10 g (65.4 mmol) of (−)-*cis*-myrtanylamine ((1*S*)-[1α,2β,5α]-2-methanamine-6,6-dimethylbicyclo[3.1.1]heptane, from Aldrich) were dissolved in 100 mL of methanol. To this solution were added 27 g of K_2CO_3 (3 mequiv) and 55 g of methyliodide (2 mequiv). The mixture was stirred for a few minutes and then kept static for 12 h at room temperature in the absence of light. The reaction mixture was filtered, and the solid filtrate was washed with an additional 50 mL of methanol. The combined methanol solutions were heated at about 323 K in a rotavapor. A white solid is formed in the flask which is then extracted with 2 portions each of 100 mL of $CHCl_3$. The combined $CHCl_3$ solutions, that now contain the trimethylmyrtanylammonium, were filtered again and were heated in a rotavapor until the $CHCl_3$ was evaporated. Often, a very viscous oily liquid was obtained after evaporation of the $CHCl_3$. In this case, the ammonium salt can be easily crystallized by the addition of 50 mL of diethyl ether. After the solid was formed, the crystals were washed with 200 mL of additional ether. The ether was then allowed to evaporate from the solid at room temperature in a hood. The recovered solids were recrystallized from a 9:1 tetrahydrofuran/methanol solution; 16.9 g (80% yield) of completely white crystals of the iodide salt of **I** were recovered; ^{13}C NMR δ = 23.2, 23.7, 25.6, 27.2, 31.5, 35.6, 38.2, 40.2, 47.6, 53.8, 76.9 ppm. $C_{13}H_{26}NI$ Anal. Calcd: C, 48.3; N, 4.3; H, 8.0; I, 39.3. Found: C, 47.9; N, 4.25; H, 8.16; I, 39.21.

The exchange of the iodide salt into a hydroxide was accomplished as follows: 4.2 g of the iodide salt of I (13 mmol) was dissolved in 60 mL of distilled water and passed through a 100 mL column of Amberlite IRA-400 OH anion exchange resin (140 mmol exchange capacity). The collected solution was concentrated to a total volume of 50 mL in a rotavapor at 343 K. The conversion of iodide to hydroxide was 96% based on titration of the resultant solution.

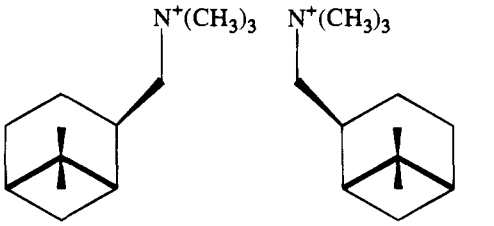

I II

Synthesis of *N,N,N*-Trimethyl (+)-*cis*-myrtanylammonium (II) Hydroxide. The synthesis of *N,N,N*-trimethyl (+)-*cis*-myrtanylammonium (**II**) was carried out by reacting (+)-*cis*-myrtanylamine with methyl iodide as described above for **I**. (+)-*cis*-myrtanylamine was prepared via hydroboration of β-pinene following the procedure of Brown et al.[15] However, in this case (+)-β-pinene ((1*R*)-6,6-dimethyl-2-methylenebicyclo[3.1.1]heptane, from Fluka) was used as starting reagent rather than (−)-β-pinene. The yield for the crude amine was 48%. After reaction with iodomethane and recrystallization, the iodide salt (7 g, 66% yield) of **II** was exchanged to the hydroxide form as described above. (+)-(*cis*)-*myrtanylamine* ^{13}C NMR δ = 20.3, 23.3, 26.2, 28.1, 33.4, 38.7, 41.6, 43.9, 45.6, 48.4 ppm.

Synthesis of *N,N,N*-Trimethyl-(1*S*,2*S*,3*S*,5*R*)-isopinocampheylammonium (III) Hydroxide. (1*S*,2*S*,3*S*,5*R*)-Isopinocampheylamine ([1α,2β,3β,5α]-2,6,6-trimethyl-3-aminebicyclo[3,1,1]heptane) was first synthesized from (+)-α-pinene by hydroboration.[15] The preparation was carried out using hydroxylamine-*O*-sulfonic acid in diglyme. Specifically, trimethylisopinocampheylammonium was synthesized here by reacting (1*S*,2*S*,3*S*,5*R*)-isopinocamphenylamine as was done to yield trimethylmyrtanylammonium and exchanged to the hydroxide form as described above. *Isopinocampheylamine* ^{13}C NMR δ = 20.9, 23.3, 28.0, 34.0, 38.3, 39.6, 42.0, 48.1, 48.7, 50.7 ppm. *Trimethylisopinocampheylammonium* ^{13}C NMR 23.1, 24.1, 26.8, 29.3, 30.9, 36.8, 38.3, 40.5, 48.2, 51.5, 73.9 ppm. $C_{13}H_{26}NI$ Anal. Calcd: C, 48.3; N, 4.3; H, 8.0; I, 39.3. Found: C, 48.4; N, 4.12; H, 8.05.

***N,N,N*-Trimethyltricyclo[5.2.1.0^{2,6}]decaneammonium (IV).** The tricyclodecane derivative (**IV**) was supplied by S. I. Zones and Y. Nakagawa of Chevron Research and Technology Company, Richmond, California.

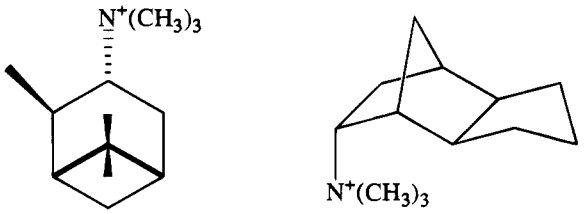

III IV

Zeolite Synthesis. The borosilicate molecular sieve CIT-1 was synthesized from reaction mixtures of composition:

$$50SiO_2{:}xB_2O_3{:}10ROH{:}5NaOH{:}yH_2O$$

where R is *N,N,N*-trimethyl-(−)-*cis*-myrtanylammonium (**I**), with $0.8 < x < 1.7$ and $2500 < y < 10\,000$. A typical synthesis of CIT-1 was carried out with $x = 1$ and $y = 3000$ (SiO_2/B_2O_3 ratio of 50 and a H_2O/SiO_2 ratio of 60). For this composition, 0.2 g of sodium borate decahydrate ($Na_2B_4O_7{\cdot}10H_2O$) and 0.2 g of NaOH were dissolved in a solution obtained by combining 29 mL of a 0.35 M solution of ROH and 26 mL of distilled water. After the solids were completely dissolved, 3 g of fumed silica (Cab-O-Sil grade M-5) were added, and the mixture blended until an homogeneous gel was obtained. The mixture was sealed in pure-silica glass tubes (25 mm i.d., 100 mm long approximately 85% filled with the gel) and heated statically in convection ovens at 423 K for 3−5 weeks. After the crystallization, the solid product was recovered by filtration and was dried in air at room temperature. To remove the organic molecules occluded inside the zeolite pores, the sample was heated at a rate of 5 K min^{-1} to 923 K in air and kept at this temperature for 4 h. Treatment of the calcined sample of CIT-1 with 0.01 N HCl (solid/liquid ratio of 1g/100 mL) for 24 h removes the B that is incorporated in the framework.[16] Insertion of aluminum into the framework positions was accomplished by reflux of the HCl treated sample in an $Al(NO_3)_3$ solution (CIT-1: $Al(NO_3)_3{\cdot}9H_2O{:}H_2O$ ratio = 1:2:50 by weight)[17] for 12 h. The CIT-1 samples treated with $Al(NO_3)_3$ will be denoted Al-CIT-1.

Analytical. X-ray powder diffraction (XRD) patterns were collected on a Scintag XDS 2000 diffractometer using Cu-Kα radiation and a solid-state Ge detector. The diffraction profiles were scanned over the range of $2° < 2\Theta < 50°$ in steps of 0.02° with a count time of 15 s at each point. Fluorophologopite mica (Standard Reference Material 675, National Bureau of Standards) was used as an external standard. Fourier-transform infrared (FTIR) spectroscopy was carried out on a Nicolet System 800. The samples were prepared using the KBr pellet technique. Thermogravimetric analyses (TGA) were performed in air on a DuPont 951 thermogravimetric analyzer with a heating rate of 5 K min^{-1}. Nitrogen adsorption isotherms were collected at 77 K on an Omnisorp 100 analyzer. The scanning electron micrographs (SEM) were recorded on a Camscan series 2-LV scanning electron microscope. Elemental analyses were performed at Galbraith Laboratories Inc., Knoxville, TN.

(15) Brown, H. C.; Kim, K. W.; Srebnik, M.; Singaram, B. *Tetrahedron* **1987**, *43*, 4071−4078.

(16) de Ruiter, R.; Kentgens, A. P. M.; Grootendorst, J.; Jansen, J. C.; Van Bekkum, H. *Zeolites* **1993**, *13*, 128−138.

(17) Van Nordstrand, R. A.; Santilli, D. S.; Zones, S. I. In *Synthesis of Microporous Materials*; Occelli, M. L., Robson, H., Eds.; Van Nostrand Reinhold: New York, 1992; Vol. 1, p 373.

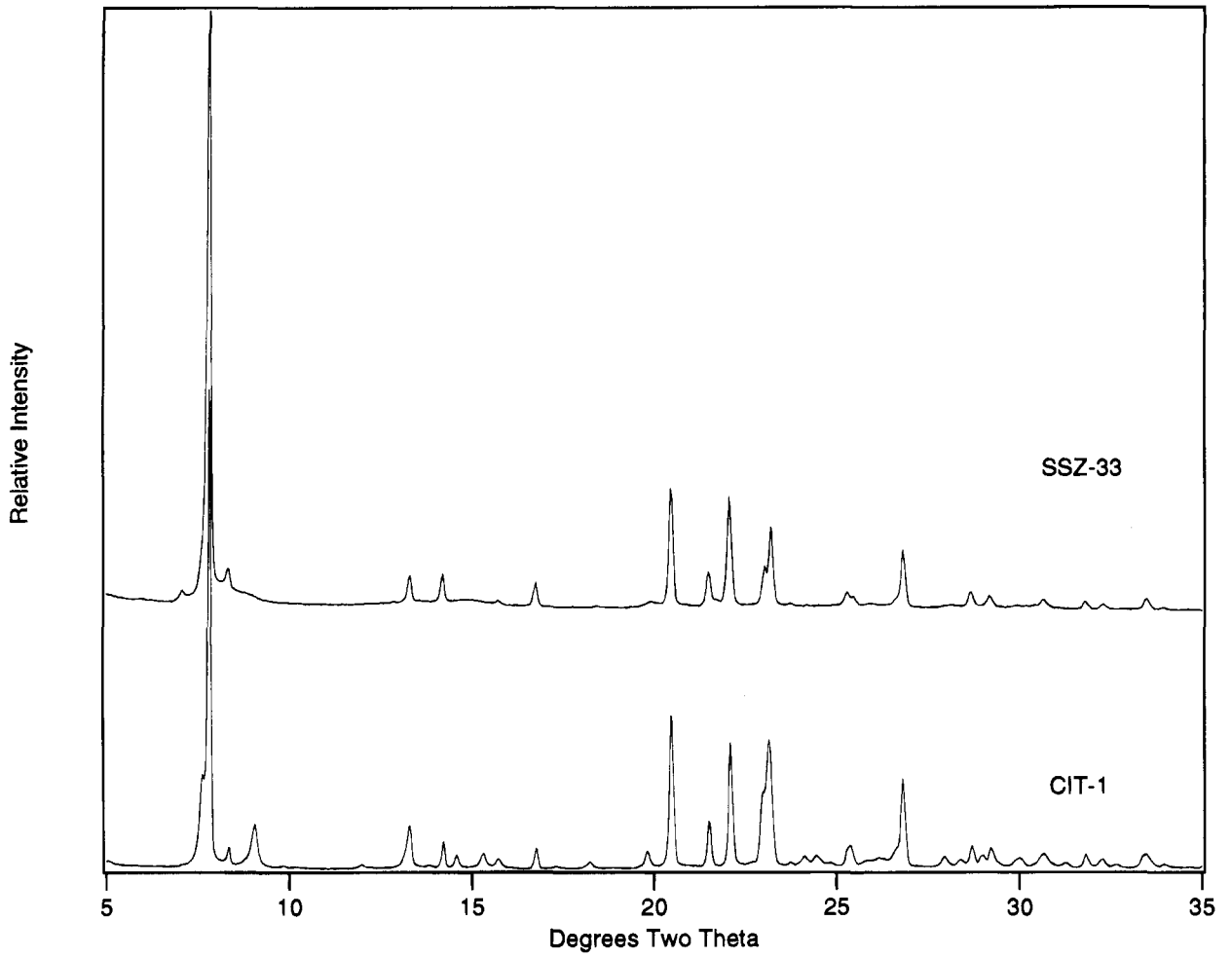

Figure 1. X-ray powder diffraction patterns of zeolites SSZ-33 and CIT-1 (Cu Kα radiation, $\lambda = 1.5460$ Å).

Liquid ^{13}C NMR spectra were collected on a GE 300 NMR QE Plus spectrometer. Solid-state NMR spectra were obtained on a Bruker AM 300 spectrometer equipped with a Bruker cross-polarization, magic angle spinning (CP/MAS) accessory. All samples were packed into ZrO_2 rotors. The ^{13}C MAS and CP/MAS−NMR spectra (75.5 MHz) were recorded with a pulse length of 4 μs and a spinning rate of 3 kHz and were referenced to an adamantane standard (downfield resonance at 38.4 ppm). ^{29}Si NMR spectra (59.63 MHz) were collected using MAS and CP/MAS with a spinning rate of 2.2−3 KHz and were referenced to a tetrakis(trimethylsilyl)silane standard (TMS, downfield resonance at −10.05 ppm). The sample used for ^{29}Si MAS−NMR was steamed at 1023 K for 3 days in air. The air stream was bubbled in a 0.1 M NH_4F aqueous solution at room temperature before contact with the zeolite sample. The ^{13}C and ^{29}Si NMR spectra are reported referenced to TMS. The ^{27}Al MAS−NMR spectra (78.2 MHz) were recorded using MAS at a spinning rate of 5 kHz and were referenced to a 1 M aqueous aluminum nitrate solution (resonance at 0 ppm). The ^{11}B MAS−NMR spectra (96.3 MHz) were obtained at a spinning rate of 4 kHz and were referenced to an aqueous solution of 1 M boric acid (resonance at 0 ppm).

Synchrotron X-ray powder diffraction data ($\lambda = 1.30042(2)$ Å) were collected at Brookhaven National Laboratory at the X7A beam line. The diffraction profile was scanned over the range of $2° < 2\Theta < 60°$ in steps of 0.01° with a count time of ~2 s at each point. Before recording the XRD pattern, the CIT-1 sample was calcined at 923 K, treated with HCl (*vide supra*), and exposed to a flowing stream of N_2 containing $SiCl_4$ vapors (see Li *et al.*[18] for details of this procedure) at 823 K. The sample was dried at 473 K before packing in a 1 mm o.d. glass capillary.

The acidic properties of Al-CIT-1 and ZSM-5 were characterized using temperature programmed desorption (TPD) of ammonia. The experiments were carried out on a flow-type apparatus equipped with a fixed-bed and thermal conductivity detector. Approximately 300 mg of the sample were activated in a helium flow at 773 K for 1 h. Pure ammonia, with a flow rate of 50 cm^3 min^{-1}, was then passed through the sample at 423 K for 30 min. The sample was subsequently purged with He at the same temperature for 1.5 h to remove the physisorbed ammonia. The TPD was performed under helium flow of 100 cm^3 min^{-1} from 423 K to 873 K with a heating rate of 10 K min^{-1}.

(18) Li, H. X.; Chen, C. Y.; Annen, M. J.; Arhancet, J. P.; Davis, M. E. *J. Mater. Chem.* **1991**, *1*, 79−85.

Catalysis

The catalytic activity of zeolite samples in the *n*-butane cracking reaction was determined using a flow type system equipped with a fixed-bed reactor. Prior to the cracking experiments, 200 mg of the sample were dehydrated *in situ* in the reactor by a helium flow of 5 L h^{-1} at 873 K, after heating from room temperature at a heating rate of 5 K min^{-1}. A gaseous mixture of *n*-butane and helium (20% vol *n*-butane) was used. The reaction was conducted at 783 K and atmospheric pressure with a total gas flow of 2 L h^{-1}. The reactant and products were analyzed with an on-line gas chromatograph using a flame ionization detector and a 50 m capillary column that contained cross-linked methyl silicone gum as stationary phase.

Results and Discussion

Structure of CIT-1. The formation of a new molecular sieve that we have denoted as CIT-1 was accomplished using a borosilicate gel and *N,N,N*-trimethyl-(−)-*cis*-myrtanyl-ammonium (**I**) as the structure-directing agent.[19] The XRD pattern of a calcined sample of CIT-1 (Si/B = 16) (Figure 1) reveals many similarities to the XRD pattern of SSZ-33 (Figure 1) indicating that it may be closely related to the structure of SSZ-

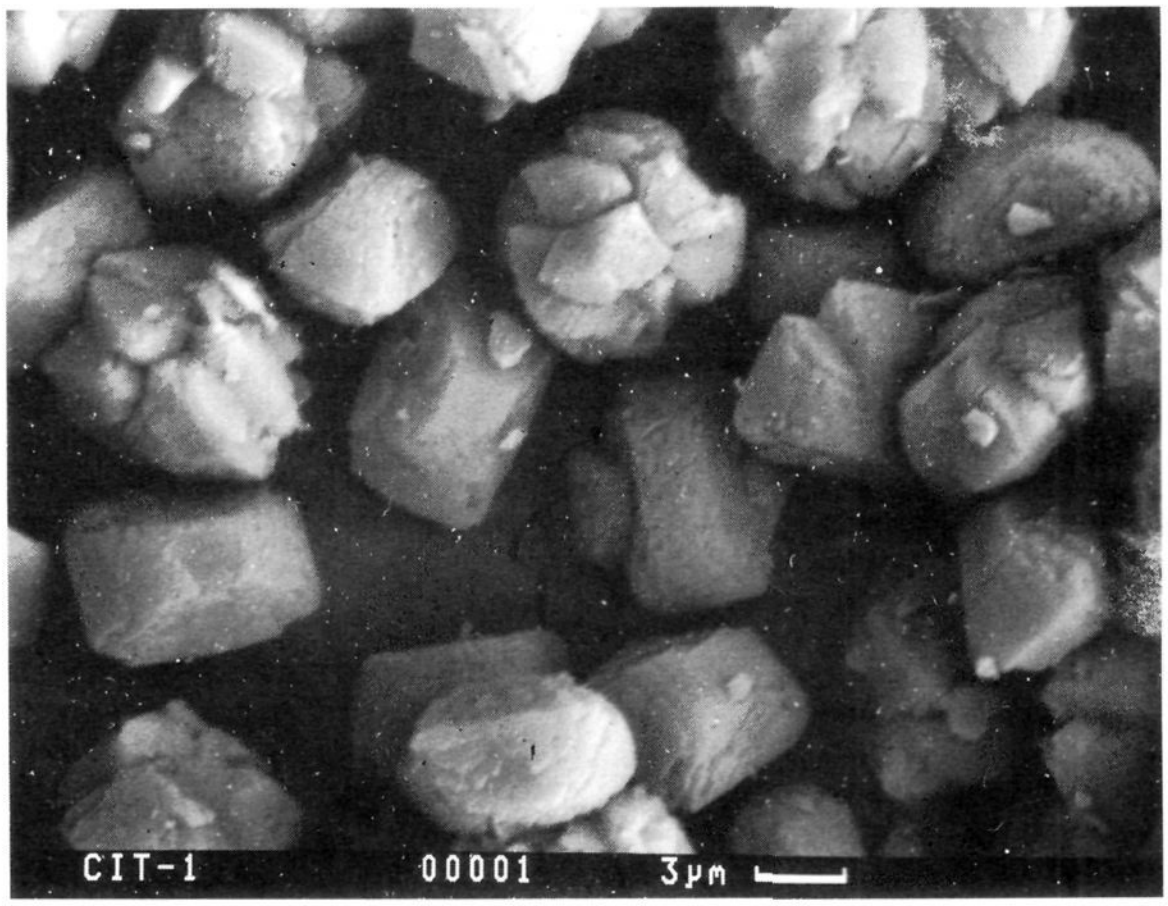

Figure 2. Scanning electron micrograph of zeolite CIT-1 (a, top) and of zeolite SSZ-33 (b, bottom).

33. However, the pattern of CIT-1 contains more reflections than the SSZ-33 pattern. The additional reflections could be the result of a higher degree of long-range order in the structure of CIT-1 than in the structure of SSZ-33, or it could be the result of the presence of other crystalline phases in the product. The SEM of CIT-1 (Figure 2a) shows the morphology and size of the CIT-1 crystals (typically 3 μm × 3 μm × 6 μm). The morphology of CIT-1 is somewhat different than the morphology of SSZ-33 (Figure 2b) and on average the CIT-1 crystals are larger (compare Figure 2 (parts a and b)) than those of SSZ-33. Many of the CIT-1 crystals are also twinned, in contrast to SSZ-33 samples that normally do not reveal this behavior. However, no other morphologies other than those shown can be detected in the samples of CIT-1. Thus, it does not appear that CIT-1 is a physical mixture of more than one crystalline phase because multiple crystal morphologies are not detected. Therefore, the additional peaks in the XRD pattern of CIT-1 are more likely an indication of a higher degree of long-range order in the structure of CIT-1 compared to the structure of SSZ-33. Using results from our previous work on the structure solution of SSZ-33 and the related aluminosilicate SSZ-26, it appeared that the XRD pattern of CIT-1 was very close to the simulated XRD pattern of polymorph B of SSZ-33.[12]

All the peaks of the XRD pattern of calcined CIT-1 could be indexed with a monoclinic unit cell (Table 1). The optimized unit cell lattice parameters (a = 22.620(8) Å, b = 13.281(5) Å, c = 12.371(5) Å, β = 68.88(3)°) agree very well with the calculated unit cell parameters of polymorph B of SSZ-33 (a = 22.62 Å, b = 13.26 Å, c = 12.33 Å, β = 68.7°).[12] (Note that in this paper the standard monoclinic setting (C-centering) is used instead of the B-centered lattice used in ref 12). The systematic absences are in agreement with the highest topological symmetry of the framework proposed for polymorph B (*C2/*

(19) Lobo, R. F.; Davis, M. E., U.S. Patent Application, 1993.

Table 1. d-Spacings and Indexing for a Calcined CIT-1 Sample

d (Å)	I/I_0[a]	hkl	d (Å)	I/I_0[a]	hkl
11.50	66	001	4.13	18	420
11.26	100	110	4.02	44	510
10.57	10	200	3.87	49	313
9.75	26	201	3.84	55	403
7.38	2	111	3.75	1	330
6.69	3	201	3.69	5	222
6.64	12	020	3.64	6	602
6.39	2	311	3.59	2	421
6.22	7	310	3.51	12	223
6.06	4	202	3.45	3	511
5.77	7	002	3.34	15	402
5.62	3	401	3.32	27	040
5.28	6	400	3.19	4	041
5.11	22	312	3.14	18	241
4.86	3	402	3.11	7	620
4.48	21	222	3.08	4	204
4.33	53	130	3.05	15	530

[a] Calculated as the ratio of the peak area to the peak area of the 110 reflection.

m, no. 12). However, these data would be also consistent with space groups *Cm* or *C2*.

Single-crystal ED patterns confirm the monoclinic unit cell derived from the XRD pattern. The C-centering ($h + k = 2n$) is clearly observed in Figure 3a. The ED pattern of CIT-1 along the [0 1 1] direction (Figure 3b), which is 45° from the [0 1 0]—the 10-ring pore direction— shows that the crystal contains twins (ABCABC... and ACBACB... stacking sequences) but shows no streaking. The streaks are ubiquitous along this axis direction in the samples of SSZ-33, and they are a manifestation of the heavy stacking faults present in the SSZ-33 materials (Figure 3c).[13] The presence of ABCABC... and ACBACB... stacking sequences and the absence of streaks in the ED pattern of CIT-1 are a strong indication that the faulting is infrequent (*vide infra*). Thus, electron diffraction data are in agreement with the postulate that CIT-1 is polymorph B of SSZ-33, with a small number of faults in each crystallite.

Rietveld Refinement of CIT-1. The sample used to obtain the synchrotron X-ray powder pattern, after treatment with HCl, presented in the ^{29}Si MAS and CP/MAS NMR spectra (not shown) a peak assigned to Q^3 silicon($(Si-O)_3-Si-OH$) that was not found in the original sample. This new peak is in agreement with the premise that silanol groups are formed upon extraction of the B atoms. To reduce the number of silanol groups, the sample was then contacted with $SiCl_4$ vapors in a N_2 stream in attempts to implant Si atoms into the framework positions vacated by B. The intensity of the Q^3 peak was reduced by this treatment (not observed in the ^{29}Si MAS NMR spectrum), but it was still observable in the ^{29}Si CP/MAS–NMR spectrum. These NMR data indicate that the $SiCl_4$ treatment did indeed reduce the number of silanol groups present in the sample but did not completely eliminate them.

The general structure analysis system[20] (GSAS) was used for the refinement of the CIT-1 sample. The refinement was initiated using the atomic positions obtained from the distance least-squares optimization of polymorph B of SSZ-33 and SSZ-26 (DLS-76)[21] using Si in all T atom positions and using the maximum topological symmetry of the framework (*C2/m*, no. 12). Other crystallographic data for the refinement are summarized in Table 2.

At the initial stage of the refinement, only the background coefficients and scale factors were optimized. In the following stages, lattice parameters and then peak shape function parameters were also included in the refinement. After convergence of the refinement, the resulting residuals were Rp = 14.8%, Rwp = 22.6%. Analysis of the difference pattern showed that some peaks had smaller widths than others; the sharper peaks were systematically of the form (*hk3n*). One possibility that could explain this anisotropic broadening is that, in agreement with the ED data, there is some small amount of faulting present in the sample.

To test the effect that a small probability of faulting (p) has upon the XRD pattern, a series of simulated XRD patterns were produced using the program DIFFaX,[22] the atomic coordinates obtained from DLS-76[21] and small values of p (see Figure 4). The results from the simulations show that there is a clear effect in the width of several reflections for faulting probabilities even as low as 1%. To account for this effect in the refinement, the anisotropic broadening axis option of the GSAS program was used. A sublattice formed by the (*hk3n*) reflections, which is not affected by the broadening effect, was defined. A new parameter characterizing the differences in the peak widths between the full lattice and the sublattice was optimized. After including this new variable, the values of the residuals dropped to Rp = 12.6% and Rwp = 16.4%.

In the next stage of the refinement, the atomic positional parameters of Si and O atoms were optimized. Soft geometrical constraints were placed on the Si–O bond distances (1.61 Å). The isotropic thermal parameters (U) were not optimized at this stage of the refinement and were fixed at a value of 0.015 and 0.03 Å^2 for the Si and O atoms, respectively. The weight of the geometric constrains was gradually reduced, and in the final refinement, the isotropic thermal parameters of all Si atoms (refined as one variable) and of all O atoms (also refined as one variable) were optimized. The final values of the residuals were Rp = 9.9% and Rwp = 11.9%. The atomic positional parameters and thermal parameters are presented in Table 3, and the experimental, calculated, and difference XRD patterns are shown in Figure 5. A stereoplot of the crystal structure of CIT-1 along [0 1 0] and along [0 0 1] is presented in Figure 6. The final residual electron density from a difference Fourier map was generally low (less than 1 e Å^{-3}), and no scattering matter that could be associated with atoms in the pores was found.

All the Si–O distances (Table 4) are within 2σ of the expected 1.61 Å and for each Si atom, average bond distances are in very good agreement with this value (differences are less than 0.05 Å). The minimum, maximum, and average Si–O bond distances are 1.55, 1.66, and 1.608 Å, respectively. The T–O–T angles (Table 4) range from 125° to 170° with an average of 155°. These values are within the ranges normally reported for Rietveld refinement of zeolites.[23] It is important to note that most of the long Si–O bond distances are associated with oxygen atoms placed along the mirror plane of *C2/m* (O(8), O(15), O(18), O(22), and O(23), marked with an asterisk in Table 4). This result quite possibly indicates that the real symmetry of CIT-1 does not contain this mirror plane. If the mirror planes are removed, these oxygen atoms should move away from the mirror planes to form shorter Si–O bond distances (symmetry reduced to at least *C2*). Fyfe et al.[24] have shown that ^{29}Si MAS–NMR can help to resolve issues regarding different alternatives of space groups that agree with the diffraction data. However, our attempts to use ^{29}Si MAS–NMR

(20) Larson, A. C.; Von Dreele, R. B. *General Structure Analysis System*; Los Alamos National Laboratory: Los Alamos, NM, 1994.

(21) Baerlocher, C.; Hepp, A.; Meier, W. M. *DLS-76*, In Institut für Kristallographie und Petrographie, ETH: Zurich, 1976.

(22) Treacy, M. M. J.; Deem, M. W.; Newsam, J. M. *Proc. R. Soc. London A* **1991**, *433*, 499.

(23) Petrovic, I.; Navrotsky, A.; Zones, S. I.; Davis, M. E. *Chem.Mater.* **1993**, *5*, 1805–1813.

(24) Fyfe, C. A.; Gies, H.; Kokotailo, G. T.; Pasztor, C.; Strobl, H.; Cox, D. E. *J. Am. Chem. Soc.* **1990**, *111*, 2470–2474.

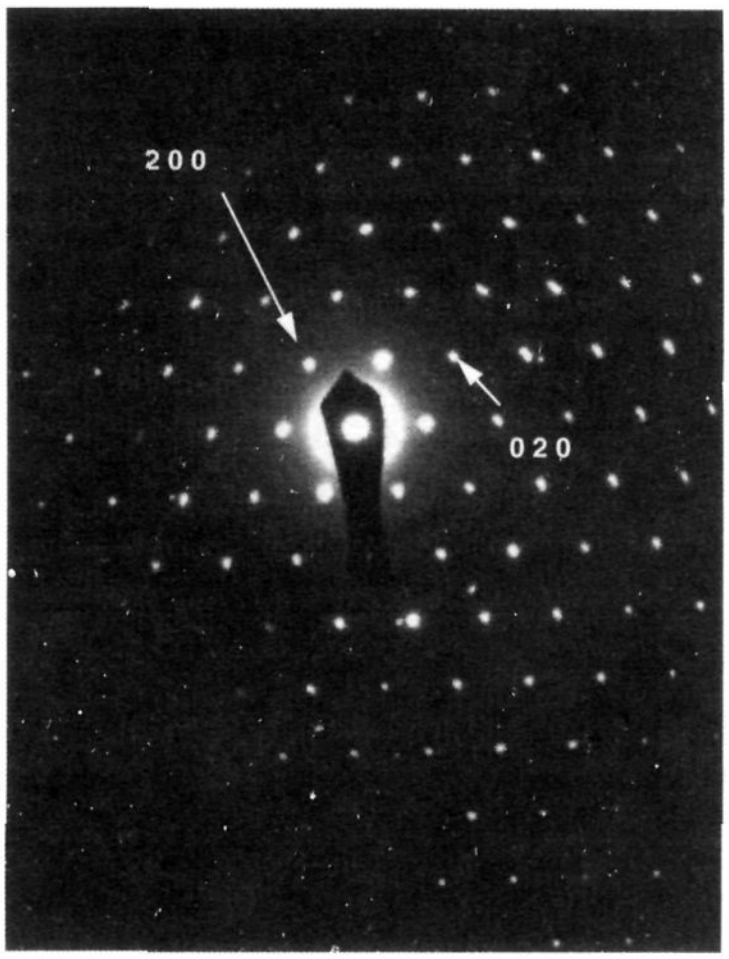

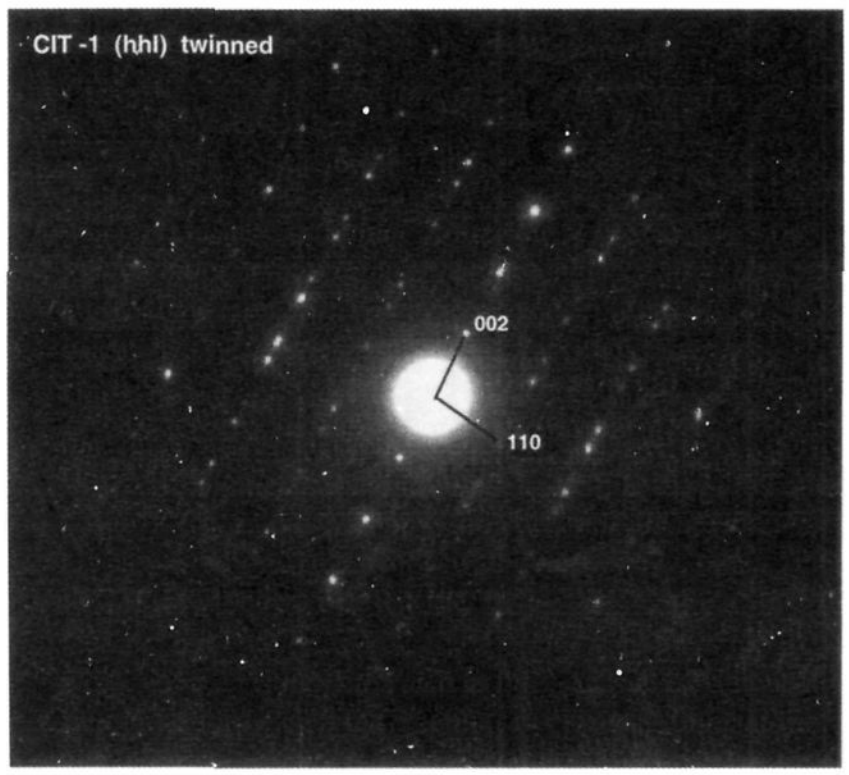

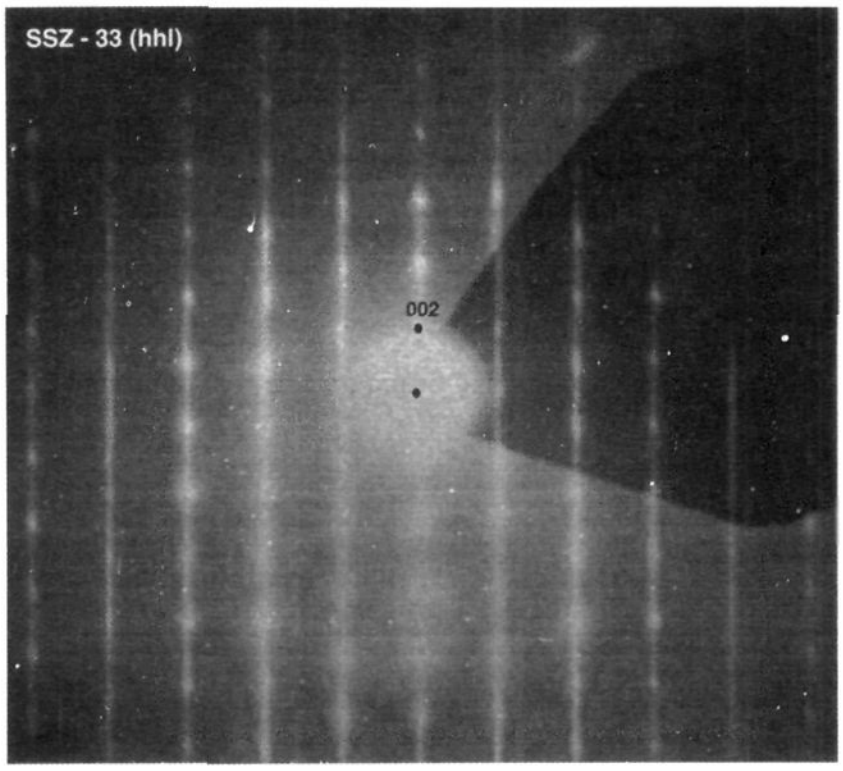

Figure 3. Electron diffractogram of zeolite CIT-1 along [001] (a) and along [011] (b). The effect of faulting on the ED pattern of SSZ-33 along the equivalent [011] is given for comparison in (c).

Table 2. Crystallographic Data

data collection temp	298 K
wavelength	1.30042(2) Å
profile range	6−60°
step scan increment	0.01°
space group	*C2/m* (no. 12)
a	22.6242 (1) Å
b	13.3503 (4) Å
c	12.3642 (6) Å
β	68.913 (4)°
no. observations	5417
no. reflcns	1085
no. uniquely defined reflcns	17
no. profile parameters	12
no. structural parameters	68
Rwp	11.9 %
Rp	9.9%

of a steamed sample to resolve the different crystallographic sites in CIT-1 were not successful (Figure 7). Although the Q^3 resonance in the spectrum has been eliminated and a small shoulder at −116 ppm can now be observed, no insights into the number of T-sites could be obtained. Reduction of the symmetry to the space group *C2* would increase the number of structural parameters to 134. Therefore, no attempts were made to lower symmetry in the refinement because only 17 uniquely defined reflections (out of 1085) can be observed in the XRD pattern. Similar limitations have been reported for other molecular sieves.[25]

The free diameters (maximum and minimum) for the 12MR channel are 6.8 Å × 6.4 Å (calculated from O(11)−O(11) and from O(18)−O(22) with an oxygen radius of 1.35 Å)[26] and for the 10MR channel are 5.1 Å × 5.1 Å (O(12)−O(21), O(9)−O(9)). These values are somewhat smaller than those observed in multidimensional 12MR pore materials like zeolite beta (7.6 Å × 6.4 Å) and faujasite (7.4 Å) and multidimensional 10MR pore materials like ZSM-5 (5.6 Å × 5.3 Å).[26] However, it is expected that combination of both pore sizes should give special catalytic properties to CIT-1.

The results from the Rietveld refinement of zeolite CIT-1 confirms the proposed topology of this material. CIT-1 is essentially the pure polymorph B of the disordered zeolite SSZ-33. The results of the refinement also indicate that CIT-1 is not completely fault-free. The overall stacking sequence of a

(25) Kennedy, G. J.; Higgins, J. B.; Ridenour, C. R.; Li, H. X.; Davis, M. E. *Solid State Nuclear Magn. Spectrosc.*, in press.

(26) Meier, W. M.; Olson, D. H. *Atlas of Zeolite Structure Types*, 3rd ed.; Butterworth-Heinemann: Stoneham, MA, 1992.

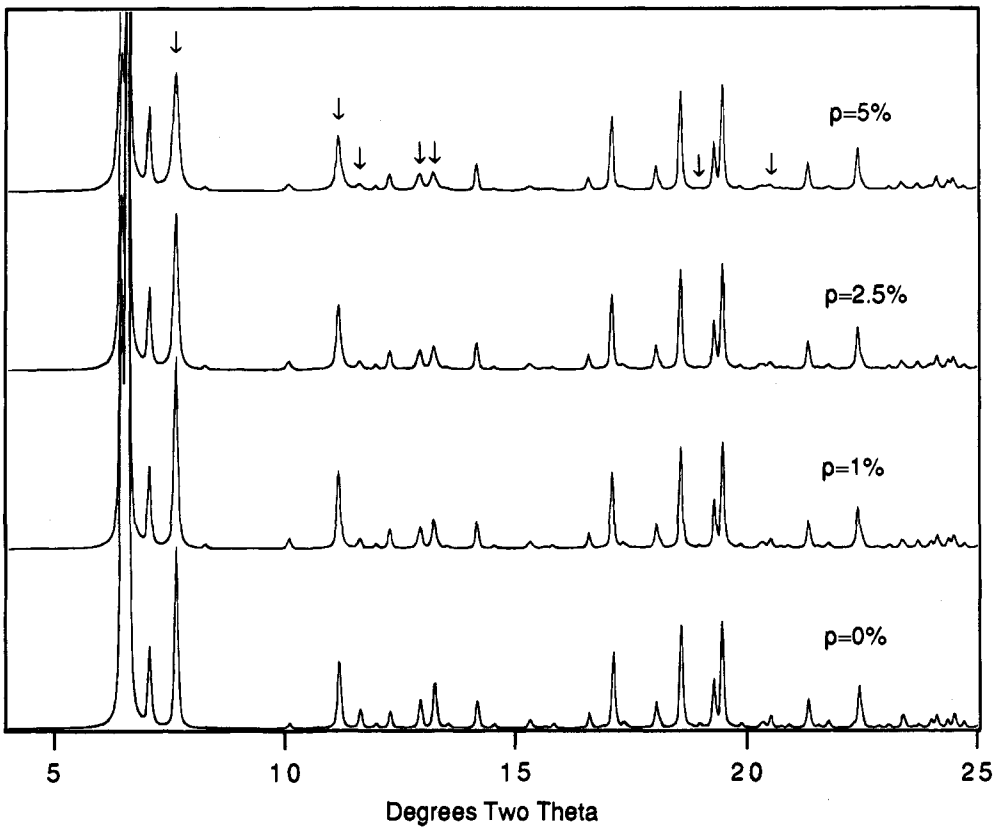

Figure 4. Effect of small values of the faulting probability p on the simulated XRD patterns of polymorph B of zeolite SSZ-33 (λ = 1.3004 Å).

Table 3. Refined Atomic Positional Parameters in Space Group *C2/m* (no. 12) and esd in parentheses[a]

atom	site	x	y	z
SI(1)	8j	0.0677(11)	0.1102(20)	0.4914(26)
SI(2)	8j	0.1567(13)	0.1889(19)	0.2510(27)
SI(3)	8j	0.0734(13)	0.1204(18)	0.7390(23)
SI(4)	8j	0.2879(12)	0.1171(19)	0.1026(24)
SI(5)	8j	0.2770(11)	0.1141(21)	0.8607(23)
SI(6)	8j	0.0738(14)	0.1195(19)	0.1043(30)
SI(7)	8j	0.1480(13)	0.1898(21)	0.8835(26)
O(8)	4i	0.0763(23)	0.0000	0.4256(55)
O(9)	8j	0.0784(22)	0.1380(29)	0.6085(37)
O(10)	8j	0.1205(20)	0.1669(31)	0.3814(35)
O(11)	4h	0.0000	0.1458(41)	0.5000
O(12)	8j	0.2185(17)	0.1200(34)	0.2009(37)
O(13)	8j	0.1097(21)	0.1569(30)	0.1860(43)
O(14)	8j	0.1728(19)	0.3005(28)	0.2109(40)
O(15)	4i	0.0852(27)	0.0000	0.7309(51)
O(16)	8j	0.0003(20)	0.1379(29)	0.8223(43)
O(17)	8j	0.1271(18)	0.1859(29)	0.7717(35)
O(18)	4i	0.3045(25)	0.0000	0.1272(62)
O(19)	8j	0.2721(17)	0.1330(31)	0.9904(36)
O(20)	8j	0.3442(18)	0.1888(30)	0.0983(42)
O(21)	8j	0.2102(19)	0.1217(35)	0.8382(39)
O(22)	4i	0.3046(29)	0.0000	0.8219(57)
O(23)	4i	0.0873(28)	0.0000	0.1087(70)
O(24)	8j	0.0837(17)	0.1783(30)	0.9900(35)

[a] The isotropic thermal parameters of the Si and O atoms converged to U_i = 0.0187(24) Å^2 and U_i = 0.018(4) Å^2, respectively.

CIT-1 crystal contains a small probability of faulting, probably close to 1% (determined by comparison to calculated XRD patterns). Analysis of the Si−O bond distances also suggest that the real symmetry of the zeolite is probably lower than *C2/m* , but no further refinement of the data was carried out in space groups of lower symmetry for reasons discussed above.

Synthesis of CIT-1. Pure samples of CIT-1 can be crystallized using a range of temperatures and chemical compositions. The temperature has a strong effect on the crystallization time.

Table 4. Interatomic Distances (Å) and Angles with esd's in Parentheses

Si(1)−O(8)	1.659(33)*	Si(5)−O(14)	1.628(35)
O(9)	1.596(35)	O(19)	1.59(4)
O(10)	1.637(33)	O(21)	1.635(34)
O(11)	1.570(24)*	O(22)	1.651(29)*
mean	1.615	mean	1.626
Si(2)−O(10)	1.55(4)	Si(6)−O(13)	1.59(4)
O(12)	1.601(35)	O(16)	1.612(35)
O(13)	1.60(4)	O(23)	1.628(25)*
O(14)	1.571(31)	O(24)	1.56(4)
mean	1.581	mean	1.598
Si(3)−O(9)	1.59(4)	Si(7)−O(17)	1.61(4)
O(15)	1.626(23)*	O(20)	1.655(33)
O(16)	1.62(4)	O(21)	1.597(35)
O(17)	1.662(34)	O(24)	1.579(34)
mean	1.624	mean	1.610
Si(4)−O(12)	1.602(33)		
O(18)	1.661(27)*		
O(19)	1.567(34)		
O(20)	1.58(4)		
mean	1.602		

Si(1)−O(8)−Si(1)	125.0(5)[a]	Si(3)−O(17)−Si(7)	133.7(3)
Si(1)−O(9)−Si(3)	154.9(3)	Si(4)−O(18)−Si(4)	140.0(5)[a]
Si(1)−O(10)−Si(2)	155.0(4)	Si(4)−O(19)−Si(5)	156.6(3)
Si(1)−O(11)−Si(1)	145.0(5)[a]	Si(4)−O(20)−Si(7)	135.5(3)
Si(2)−O(12)−Si(4)	142.0(4)	Si(5)−O(21)−Si(7)	136.6(3)
Si(2)−O(13)−Si(6)	170.0(4)	Si(5)−O(22)−Si(5)	135.0(5)[a]
Si(2)−O(14)−Si(5)	151.0(4)	Si(6)−O(23)−Si(6)	157.0(5)[a]
Si(3)−O(15)−Si(3)	162.0(5)[a]	Si(6)−O(24)−Si(7)	126.3(3)
Si(3)−O(16)−Si(6)	162.3(3)	mean	155.4

[a] Distances and angles associated with an oxygen atom in a special position.

Fully crystalline product can be obtained in 8−10 days at 448 K and in 21-35 days at 423 K. However, there is a lack of reproducibility in the syntheses at 448 K, with large amounts of kenyaite (layered silicate)[27] often found in the final product. It is possible that at 448 K, the Hoffmann degradation of **I** is

Table 5. Minimum Energies (kJ) of **I** and **IV** in the Pores of Polymorph A and B of SSZ-33

	polymorph A		polymorph B	
molecule	12-ring pores	10-ring pores	12-ring pores	10-ring pores
I	−104	−38	−104	−41
IV	−104	−66	−104	−72

Table 6. Conversion of *n*-Butane at 783 K After 3 h On-Stream for Various Zeolites

sample	Si/Al	conversion, %
ZSM-5	31	85
Al-CIT-1	34	65
Al-CIT-1	60	22
zeolite beta	32	40

faster than at 423 K, and that the degradation products interfere with the synthesis of CIT-1. Most of the CIT-1 syntheses were therefore conducted at 423 K, and all the characterization data given in this paper are from samples prepared at this temperature.

Comparison of the ^{13}C CP/MAS−NMR spectrum of the as-synthesized sample of CIT-1 with the liquid ^{13}C spectrum of **I** indicates that **I** is occluded intact inside the pores of the zeolite. No other peaks are observed in the spectrum besides the ones assigned to **I**. The ^{11}B MAS spectrum of as-synthesized CIT-1 show only one peak at −3 ppm, consistent with the presence of only tetrahedrally coordinated boron in the product (Figure 8).

FTIR spectra of as-synthesized CIT-1 and SSZ-33 are essentially identical, except for small differences in the region of 1400−1500 cm^{-1} (Figure 9). These spectral features are due to differences in the IR spectra of the structure-directing agents **I** and **IV**. FTIR spectra of the calcined forms of the two zeolites show a band at 1400 cm^{-1}. This band is often found in the calcined form of borosilicate molecular sieves,[28] and it is assigned to trigonal boron formed during the calcination process. Additionally, bands at 907 cm^{-1} in the as-synthesized CIT-1 and SSZ-33 are in agreement with the presence of boron in tetrahedral coordination[29] as observed in the ^{11}B MAS−NMR spectrum (Figure 8a). After calcination, both bands shift to ~927 cm^{-1} in a manner similar to other borosilicates such as B-SSZ-24 and B-ZSM-5.[28] (The ^{11}B MAS spectrum of the calcined sample of CIT-1 (Figure 8b) also shows two boron environments that can be assigned to tetrahedral and trigonal boron, respectively, in agreement with the IR results.) The shift in this band from the as-synthesized to the calcined samples is probably due to differences in the water coordination environment of the framework boron atoms.

CIT-1 can be synthesized from gels with SiO_2/B_2O_3 ratios between 30 and 60. The SiO_2/B_2O_3 ratios of the calcined products are 32 and 72, respectively. If higher SiO_2/B_2O_3 ratios are used, the product often contains small amounts of SSZ-31.[30] No crystalline materials are obtained if B is absent from the synthesis gel. The formation of SSZ-31 at high SiO_2/B_2O_3 ratios is in agreement with results of Nakagawa[30] and Zones and Nakagawa,[31] who have shown that several structure-directing agents that form SSZ-33 zeolites at SiO_2/B_2O_3 ratios of 30 also form SSZ-31 at high SiO_2/B_2O_3 ratios. At SiO_2/B_2O_3 ratios below 30, CIT-1 forms, but is contaminated with layered oxide impurities. The layered, sodium silicate, kenyaite was clearly observed in the XRD pattern of all the samples that were synthesized with SiO_2/B_2O_3 ratios of 25. The formation of layered silicates for syntheses using sodium borate as a source of boron have been observed for other high-silica materials.[17,31] Synthesis gels with SiO_2/B_2O_3 ratios below 25 were not investigated. We were also unable to synthesize any crystalline product if the borate was substituted by sodium aluminate or by aluminum nitrate when **I** was used as the structure-directing agent (even after several months of heating). Similar results have been reported by Zones and Nakagawa[31] for the synthesis of SSZ-33.

The presence of a small amount of sodium is necessary for the synthesis of CIT-1. If boric acid is used instead of sodium borate, and no other source of sodium is added to the synthesis gel, no crystalline material is formed. SiO_2/NaOH ratios of 5−10 are typical for most of the syntheses. Higher sodium concentrations, as it has been observed for zeolite ZSM-12,[32] promote the nucleation of layered materials. Only small amounts of Na (less than 0.4%) are detected in the calcined samples.

Small amounts of as-synthesized B-zeolite beta (borosilicate analogue of zeolite beta) are found to promote the nucleation of CIT-1. The B-zeolite beta is a better promoter than seed crystals of CIT-1. The reasons for this behavior are not understood at this time.

It is important to emphasize that none of the effects discussed above—temperature, sodium or boron concentration, and the use of CIT-1 or zeolite beta as nucleation promoters—have any noticeable affect on the fault probability (as observed by X-ray powder diffraction). This is an indication that the long-range order observed in CIT-1 is related primarily to the structure-directing agent **I** and not to any of the other inorganic components in the synthesis gel.

What is special about **I** that promotes the formation of the ordered polymorph B of SSZ-33? First, a test to observe whether this selectivity is related to the chirality of **I** was performed. To do so, the enantiomorph of **I**, namely **II**, was prepared, and the following two syntheses were carried out: one using only **II**, and a second with equimolar amounts of **I** and **II** (racemic). The products of these two syntheses are indistinguishable—by XRD—from the CIT-1 sample prepared using **I**. The results from the first experiment are not surprising and imply that the selectivity of **I** toward the formation of polymorph B is not correlated with chirality. This is expected because neither polymorph A or B of SSZ-33 is chiral, and therefore their interactions with each enantiomorph of the organic structure-directing agent (**I** or **II**) should be the same. The result from experiment two indicates that intermolecular interactions between organic molecules are probably *not* involved in the step(s) that define the layer ordering in CIT-1. If this were the case, then interactions between two molecules of **I** (or two of **II**) should be different than interactions between a molecule of **I** and **II**. A second possibility for the structure-directing effect of **I** on CIT-1 is that the selectivity for an ordered layer sequence in CIT-1 is related to the myrtanyl, polycyclic group. If this were the case, it is expected that **III**, an isomer of **I**, would also form CIT-1. The product of a zeolite synthesis using **III** at similar conditions to those used above gives neither CIT-1, or SSZ-33, but SSZ-31. Zeolite SSZ-31 has been prepared with a variety of organocations of approximately

(27) Beneke, K.; Lagaly, G. *Am. Min.* **1983**, *68*, 818−826.
(28) Lobo, R. F.; Davis, M. E. *Microporous Mater.* **1994**, *3*, 61−69.
(29) de Ruiter, R.; Jansen, J. C.; Van Bekkum, H. *Zeolites* **1992**, *12*, 56−62.
(30) Nakagawa, Y.; Zones, S. I. In *Synthesis of Microporous Materials*; Occelli, M. L., Robson, H., Eds.; Van Nostrand Reinhold: New York, 1992; Vol. 1, pp 222−239.
(31) Zones, S. I.; Nakagawa, Y. *Microporous Mater.* **1994**, *2*, 543−555.
(32) Goepper, M.; Li, H. X.; Davis, M. E. *J. Chem. Soc., Chem. Commun.* **1992**, 1665−1666.

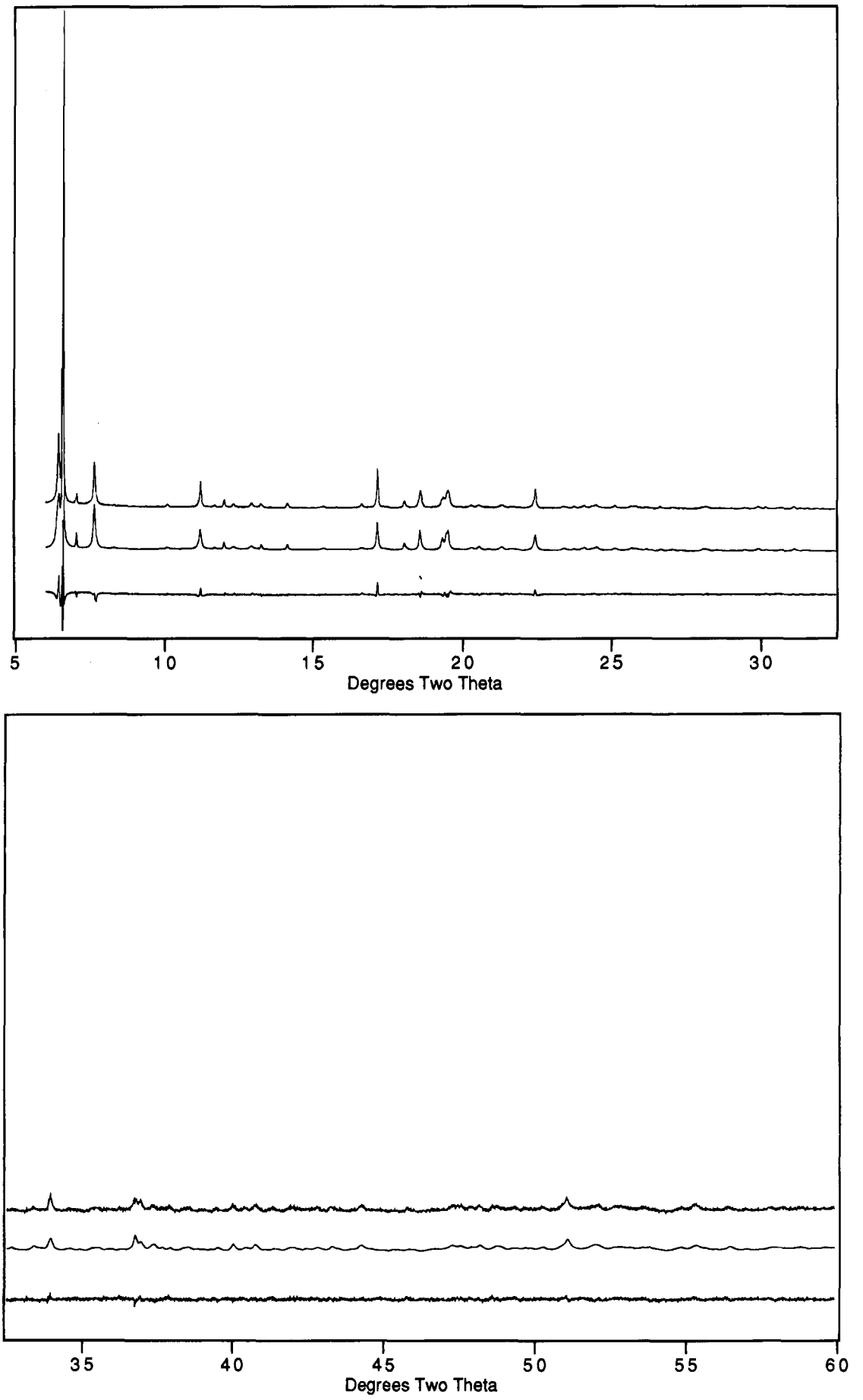

Figure 5. Observed (upper), calculated (middle), and difference (lower) profiles for synchrotron XRD patterns of zeolite CIT-1 (λ = 1.3004 Å). The intensity scale has been increased eight times for the section between 32−60° 2Θ.

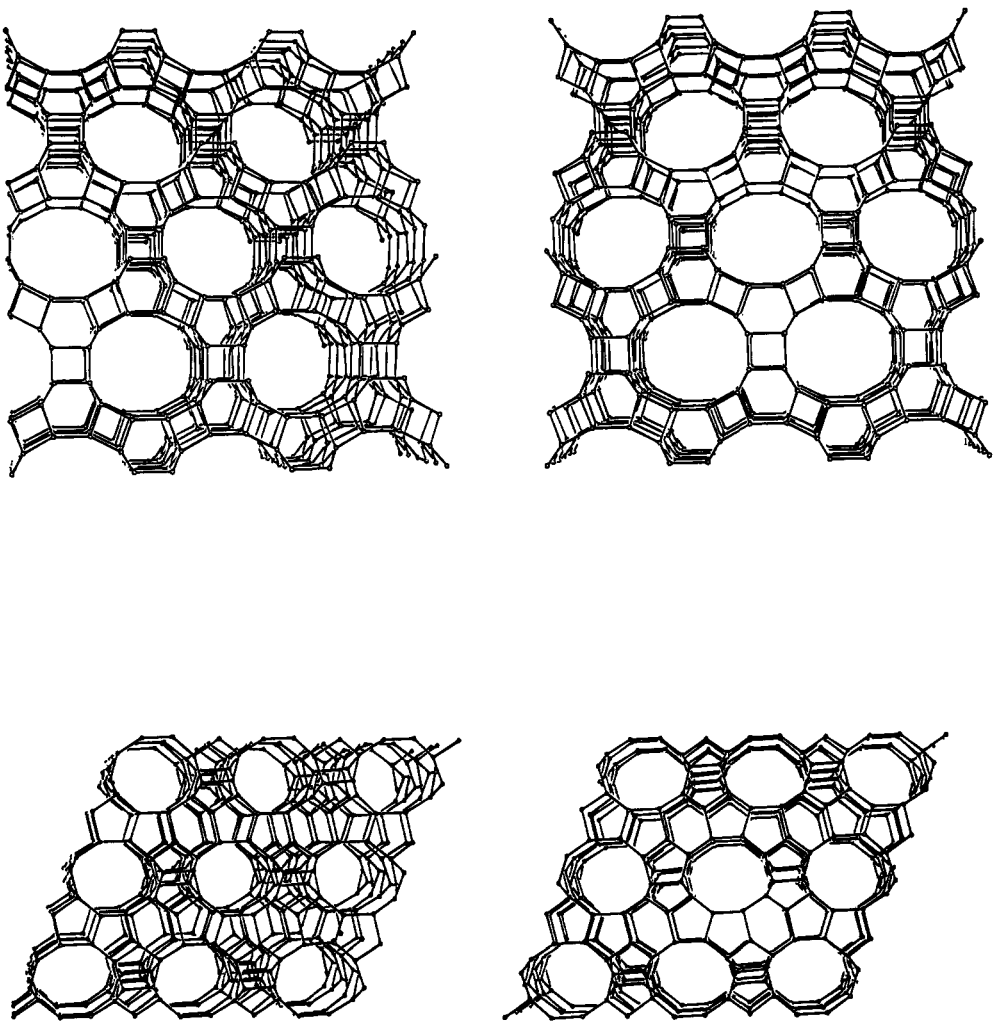

Figure 6. Stereoplot of the framework structure of CIT-1 view along [001], i.e., the 12MR channels (top), and viewed along [010], i.e., the 10MR channels (bottom). The oxygen atoms have been omitted for simplicity.

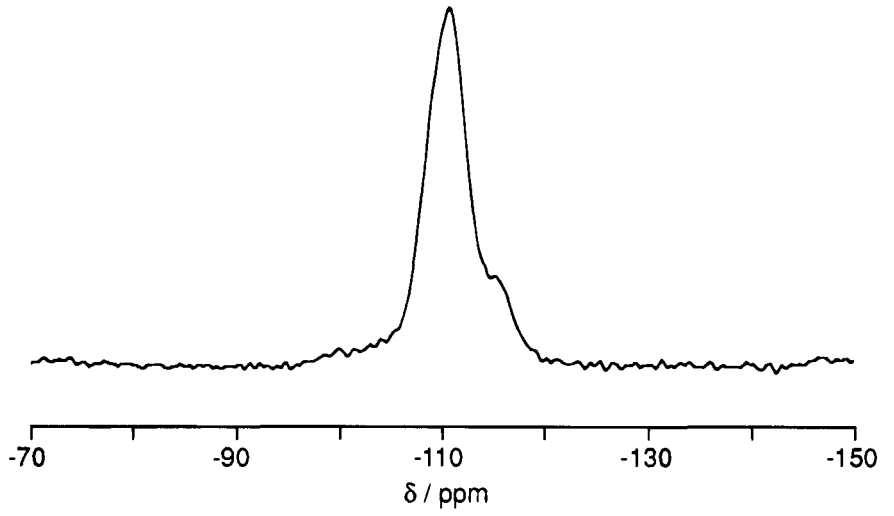

Figure 7. ^{29}Si MAS−NMR spectrum of CIT-1 after steaming.

cylindrical shape.[30] The crystallization of SSZ-31 using **III** is then understandable in terms of the geometry of this organic molecule. In **III**, the trimethylammonium group is diagonally opposite to the two methyls of the cyclobutane ring of the pinane group. Thus, the molecule is approximately cylindrical in shape and can direct the formation of SSZ-31. This result indicates that the selectivity of **I** is not due to the shape of the polycyclic myrtanyl group alone. The geometry of the complete molecule is required to achieve the long-range order observed in CIT-1.

Further insight into the structure-directing effects of **I** can be obtained by comparing the molecules that form SSZ-33 to those that form CIT-1. SSZ-33 can be synthesized using a variety of structure-directing agents that have a wide diversity of shapes. Although SSZ-33 is normally synthesized using the tricyclo[5.2.1.$0^{2,6}$]decane derivative **IV**,[5] the synthesis of SSZ-33 has also been reported using molecules **V**−**VIII**.[31] Thermogravimetric analyses of SSZ-33 synthesized with **IV** show two stages of weight loss: one stage between 298 and 573 K

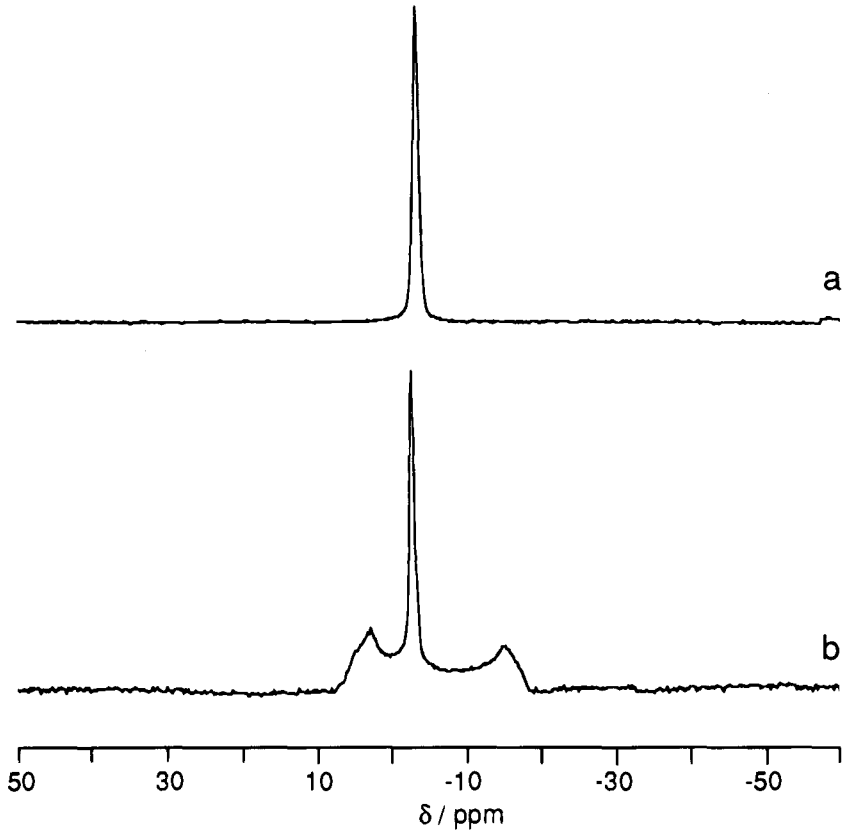

Figure 8. ^{11}B MAS NMR spectrum of CIT-1 in the (a) as-synthesized and (b) calcined forms.

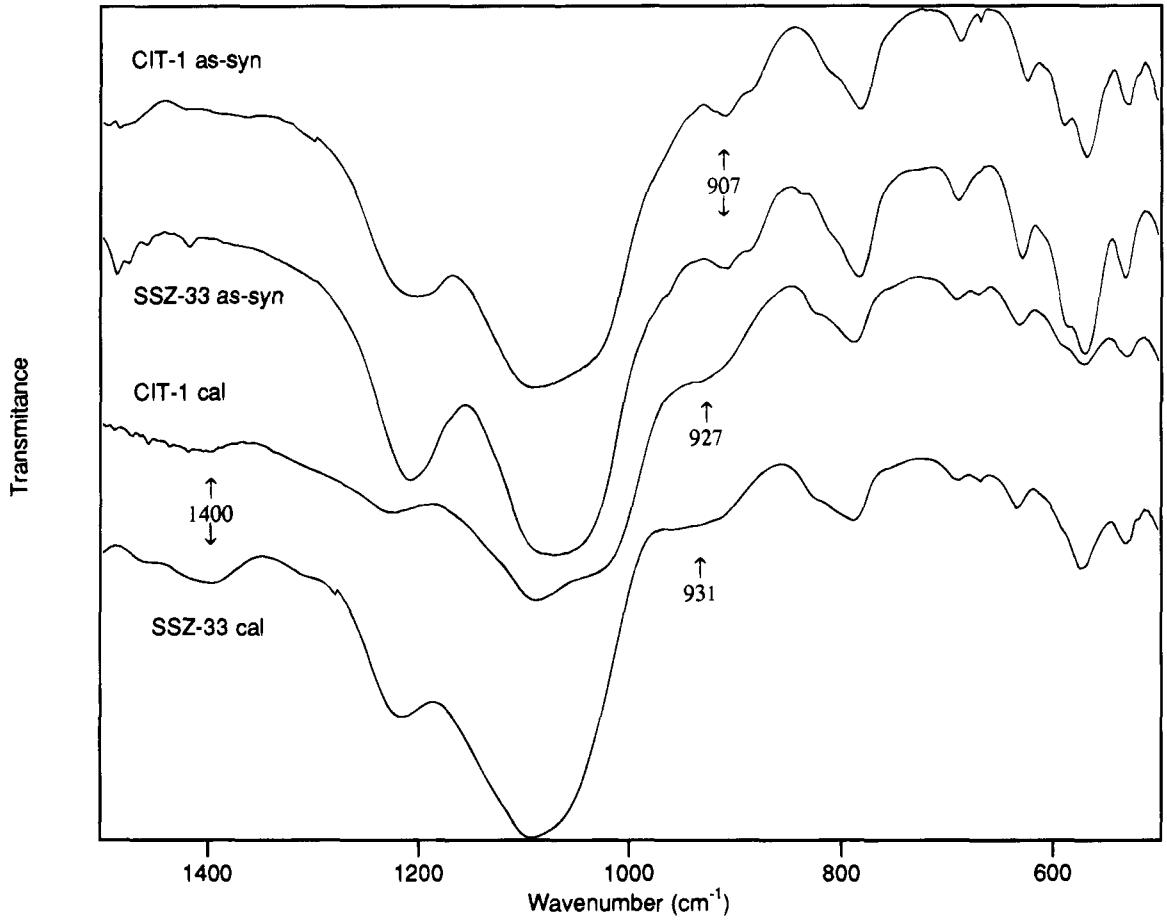

Figure 9. FTIR spectra of as-synthesized samples of CIT-1 and SSZ-33 (top) and the calcined samples of CIT-1 and SSZ-33 (bottom).

at 0.4% which is assigned to water desorption, and a second stage between 573 and 923 K with a weight loss of 18.2% that is assigned to the pyrolysis and combustion of **IV**. The second weight loss corresponds to 3.9 molecules of **IV** ($C_{13}H_{26}N$) per

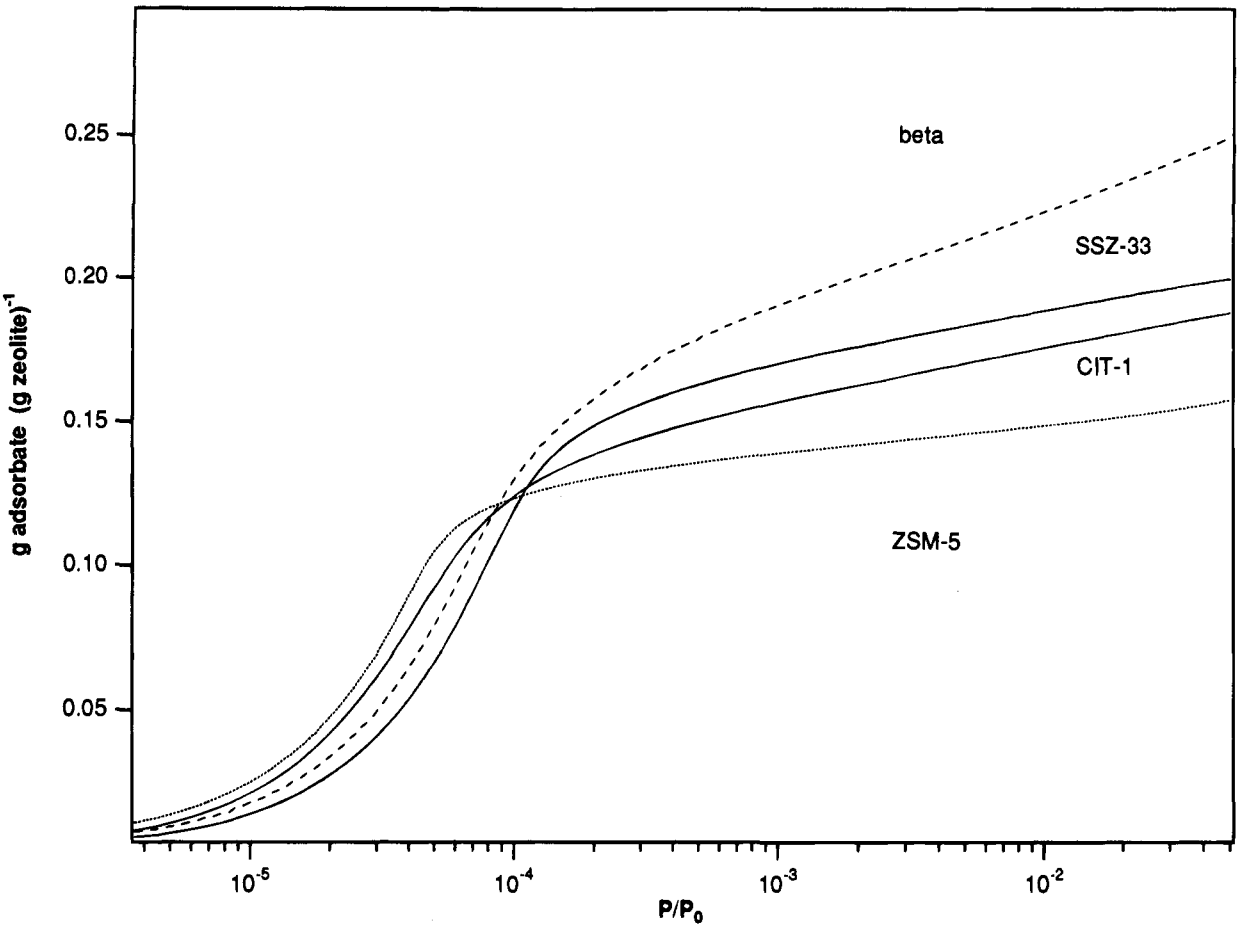

Figure 10. Physical adsorption isotherms of N_2 at 77 K for CIT-1, SSZ-33, ZSM-5, and zeolite beta.

unit cell of SSZ-33. The TGA of CIT-1 also shows two stages of weight loss. For CIT-1, the weight loss between 298 and 573 K is 1.5% and between 573 and 923 K is *only* 14.5% (**I**: $C_{13}H_{26}N$). The high-temperature weight loss from CIT-1 corresponds to 2.9 molecules of **I** per unit cell. Given the similarity in the chemical composition of **I** and **IV**, this difference is significant. The TGA results for CIT-1 indicate that the geometry of **I** is such that the molecule cannot adopt a conformation inside the void space that completely fills the pores (*vide infra*). This is unlike **IV**, which seems to adopt a conformation that fills the pores more completely. The very small water loss (only 0.4%) of SSZ-33 prepared with **IV** is also in agreement with a very efficient packing of **IV** inside the void space.

The differences in weight loss at high temperature between SSZ-33 and CIT-1 are not the result of differences in void volume or pore sizes between these two structures. The *n*-hexane adsorption capacity of CIT-1 is 0.18 mL g^{-1}(P/P_0 = 0.3), very similar to the cyclohexane adsorption capacity reported for SSZ-33 (0.20 mL g^{-1}). Additionally, physical adsorption isotherms of N_2 at 77 K for both materials are very similar (Figure 10) but are different from the isotherms obtained for multidimensional 12MR zeolites (zeolite beta) and multidimensional 10MR zeolites (ZSM-5).

De Ruiter *et al.*[29] have previously indicated that for B-substituted ZSM-5 and beta zeolites, there appears to be an approximate one-to-one correspondence between the number of positive charges of the organic cations per unit cell and the negative charges introduced to the silicate by the isomorphous substitution of B^{3+} for Si^{4+}. Similar to the results observed by de Ruiter et al. for other borosilicates,[29] it is found here for CIT-1 from chemical analysis that there are 3.3 B atoms per unit cell, in rough agreement with the three molecules of **I** per unit cell derived from TGA. The chemical analysis of SSZ-33

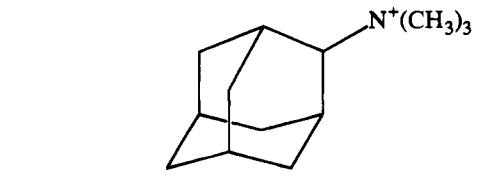

V

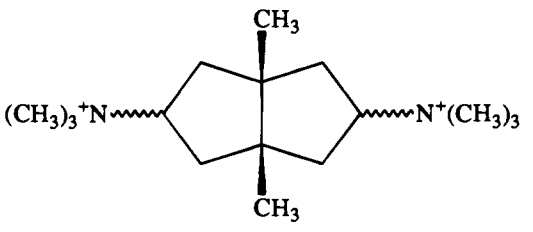

VI

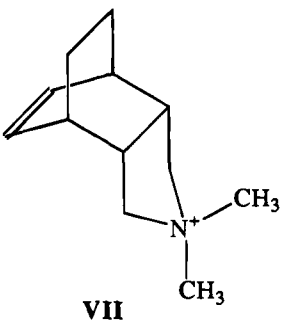

VII

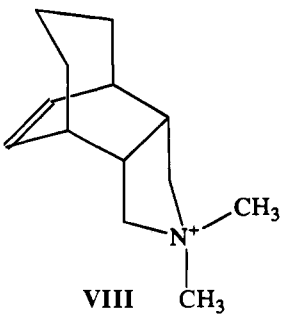

VIII

indicates that there are 3.8 B atoms per unit cell which is also in correspondence with the results derived from TGA for the number of organic molecules per unit cell.

To test further the relationships between CIT-1 and SSZ-33, syntheses were carried out using two structure-directing agents (**I** and **IV**).[14] Five different preparations were investigated using mixtures of **I** and **IV** in the molar ratios of 100:0, 75:25, 50:50, 25:75, and 0:100. The XRD patterns of the calcined samples show that there is a continuous change in the faulting probability from $p = 30\%$ (SSZ-33) synthesized using only **IV** to $p \sim 0\%$ for materials synthesized with **I** (CIT-1). These XRD patterns correlate very well with simulations using fault probabilities of $p = 30$, 22.5, 15, 7.5, and 0% and indicate that the fault probability changes linearly with the relative concentrations of the structure-directing agent (**I**). ^{13}C CP/MAS−NMR of the as-synthesized samples also show a continuous change in the NMR spectrum of **I** to the NMR spectrum of **IV**. This change, however, did not correlate linearly with the amounts placed in the synthesis gels (^{13}C CP/MAS−NMR of physical mixtures of CIT-1 and SSZ-33 were used for comparison). The nonlinear change in the amount of **I** and **IV** may be due to the preferential occlusion of **IV** over **I**, as found in the TGA experiments of pure SSZ-33 and CIT-1. Thus, it is absolutely clear that molecule **I** controls the ABCABC... stacking sequence of CIT-1.

Energy Minimization Calculations. Energy minimizations of molecules **I** and **IV** in the pores of polymorph A and B of SSZ-33 were calculated to gain some insights into the structure-directing effects of molecules **I** and **IV** on the formation of CIT-1 and SSZ-33, respectively. The objectives of the energy minimizations were to (i) find the most favorable conformation of these molecules in the zeolite pores and (ii) to determine the reasons why the trimethylmyrtanylammonium cation directs the crystallization of only polymorph B and not polymorph A. The minimizations were carried out using Cerius 3.2 software using the crystal packer module. We limited our modeling strictly to van der Waals interaction energies between organic molecules and pure-silica frameworks. Electrostatic interaction energies were not used because we do not have enough information about charge distribution in the organic molecules, the distribution of water in the pores and the distribution of B framework atoms in the zeolite as to form a realistic model. We do however expect that the key to the selectivity of **I** over **IV** for the formation of polymorph B will be captured by short-range interactions between the organic molecule and the framework. The simulations treat the zeolite framework and the organic molecule as rigid units. This is not a severe limitation for the organic molecules which, in this case, are fairly rigid. It is, nevertheless, a source of error for the framework because it has been previously shown that the framework of zeolite structures adapts to the shape and size of adsorbed organic molecules with small displacive transitions.[33−35] It is noteworthy to say that locally the geometrical differences between the pore shapes of both polymorphs are rather small. They consist mainly of differences in the positions of the O atoms that bound the 10-ring pores.

To find the energy minima, the organic molecules (one per unit cell) were placed randomly in the zeolite pores in 20 different positions. Then, the energy minimization program translated and rotated the molecule until it reached an energy minimum. The results of the minimizations are shown in Table 5. No differences between the interaction energies are observed for polymorphs A and B and with both molecules **I** and **IV** when they are contained in the 12MR pores alone. Minimum energies along the 10MR pores were consistently of lower stability for both molecules than the minimum energies along the 12MR pores. This indicates, as expected, that the organic molecules will reside along the large pores instead of along the medium ones. The interaction energy of **I** with the framework along the 10-ring pores is substantially less negative than the equivalent interaction of **IV**. Indeed, it was difficult to find a minimum energy conformation for **I** along the 10MR because the minimization routines would translate it to the 12MR pores (in contrast with **IV** for which there were several minima along the 10MR pores). This result is in agreement with the TGA of CIT-1, which indicates that the packing of **I** in the zeolite pores is more constrained than the packing of **IV**.

The results from the energy minimization calculations are not conclusive. More refined and complete computations, that eliminate most of the assumptions used here, are necessary in order to detect differences between the energetic interactions of the trimethylmyrtanylammonium cation with polymorphs A and B of SSZ-33. Further experimental investigations into the location and flexibility of **I** inside the CIT-1 pores will probably also be necessary to unravel the geometrical relationships between molecule **I** and the pore geometries of these zeolites.

Catalytic Properties of CIT-1. After treatment with the aluminum nitrate solution, the ^{27}Al MAS−NMR spectrum of Al-CIT-1(Si/Al = 35) shows two peaks at 56 and 0.5 ppm with relative areas of 6.5:1, respectively. These two peaks are assigned to Al in tetrahedral and octahedral coordination, respectively. The ^{27}Al NMR spectrum reveals that Al is incorporated in the framework (in tetrahedral coordination), and it is expected to form a strong acid site upon activation (although a second site may occur from the extraframework aluminum).

Ammonia TPD of Al-CIT-1 compares well to ZSM-5 and zeolite beta in the sense that all the TPD curves (not shown) are characterized by two desorption peaks. At this point, all that can be stated is that all the materials contain two types of acid sites (desorption peaks at 550 K and above 700 K).

The cracking of *n*-butane is used here as a test reaction for the acid catalytic properties of Al-CIT-1. The catalytic properties of Al-CIT-1 with intersecting 10 and 12MR pores are compared to the catalytic properties of zeolites ZSM-5 which has intersecting 10MR pores and zeolite beta that has intersecting 12MR pores. It is observed that all three zeolites show activity for the cracking of *n*-butane at 783 K (see Table 6). Since the number of acid sites is related to the aluminum content of the zeolite, it is not surprising that the zeolites with lower Si/Al ratios are more active. Before specific conclusions can be made concerning the differences in catalytic activity and deactivation due to coking between CIT-1, ZSM-5, and zeolite beta, further characterization of the catalytic properties are necessary. Here we wish to show only that Al-CIT-1 is catalytically active and should thus open new opportunities for acid-based, shape-selective catalysis.

Conclusions

A new borosilicate molecular sieve, CIT-1, has been synthesized. Rietveld refinement of the synchrotron XRD of CIT-1 confirms that this zeolite is essentially the pure polymorph B of the disordered zeolite SSZ-33. The presence of long range order in CIT-1 is a direct consequence of the structure-directing agent (*N,N,N*-trimethyl (−)-*cis*-myrtanylammonium (**I**)) and does not depend on temperature or the relative concentration of the inorganic components in the synthesis gel.

(33) van Koningsveld, H.; van Bekkum, H.; Jansen, J. C. *Zeolites* **1987**, *7*, 564−568.
(34) van Koningsveld, H.; Tuinstra, F.; van Bekkum, H.; Jansen, J. C. *Acta Crystallogr., Sect. B* **1989**, *45*, 423−431.
(35) van Koningsveld, H.; Jansen, J. C.; van Bekkum, H. *Zeolites* **1990**, *10*, 235−242.

The fault probability of the SSZ-33 type of materials can be controlled using mixtures of structure-directing agents **I** and **IV**. The results from preliminary energy minimization calculations of **I** inside the polymorph A and polymorph B of SSZ-33 revealed no conclusive information. No preference for the incorporation of **I** inside either of the two polymorphs is detected. Treatment of CIT-1 with aluminum nitrate transforms CIT-1 into an active catalyst for the cracking of *n*-butane.

Acknowledgment. We are grateful to Chevron Research and Technology for financial support. We thank C. Y. Chen and B. Adair who carried out the catalytic experiments with CIT-1, ZSM-5, and zeolite beta. We thank M. Pan from Arizona State University and I. Chan from Chevron Research and Technology Co. for taking the ED patterns of CIT-1. We acknowledge Y. Nakagawa and S. I. Zones for supplying the cyclodecane derivative and for helpful discussions. We acknowledge D. E. Cox for assistance in collecting the synchrotron data. The XRD data were collected at X7A beam line, National Synchrotron Light Source, Brookhaven National Laboratory, which is supported by the Department of Energy, Division of Material Sciences and Division of Chemical Sciences. We thank J. B. Higgins, from Mobil Central Research, for his advise in carrying out the Rietveld refinement.

JA943848U